

Diffusion Kurtosis Imaging (DKI) Reconstruction - Linear or Non-Linear?

J. Zhuo^{1,2}, J. Simon², and R. Gullapalli¹

¹Radiology, University of Maryland School of Medicine, Baltimore, MD, United States, ²Electrical & Computer Engineering, University of Maryland College Park, College Park, MD, United States

Introduction: Diffusion Kurtosis Imaging (DKI)¹ which measures the non-Gaussian behavior in diffusion has shown great potential as being a more sensitive marker in characterizing neural tissues compared to conventional DTI^{2,3}. Processing for DKI originally used nonlinear least squares (NLS) methods which were inefficient and processing time of one hour on a fast computer was not unusual^{1,4}. Later, fast DKI fitting method (fDKI)⁵ was proposed which reduced the image reconstruction time to seconds by using an explicit formula to calculate D_{app} and K_{app} when only 2 non-zero b-values were acquired, with the assumption that diffusion directions remained invariant between the different diffusion sensitivities. Similar to DTI, the DKI model could also be linearized and fit for both the Diffusion Tensor and Kurtosis Tensor directly through linear equations as described by Tabesh et al.⁶ with reconstruction times comparable to DTI reconstruction. Although the NLS approach may provide more accurate results, real-time reconstruction is critical in the clinical setting so linear methods are highly preferred. In this study DKI derived maps from both linear and non-linear least squares approaches from a clinically relevant short imaging protocol (using 2 b-values) were compared with 'gold standard' dataset that was obtained using five different diffusion sensitivities (5 b-values) to assess their performance.

Methods: Imaging: DKI data were collected on an adult male Sprague-Dawley rat. Imaging was performed on a Bruker Biospec 7T scanner with a 4-channel surface receiver coil. Diffusion weighted images were acquired with single shot spin-echo echo-planar imaging (EPI) sequence. A Bruker standard encoding scheme of 30 gradient directions was used with $\delta/\Delta=4/20$ ms. Five non-zero b-values: 500, 1000, 1500, 2000, 2500 s/mm² were acquired for each direction following five images acquired at b = 0 s/mm². FOV = 3.0 × 3.0 cm², matrix resolution = 128 × 128, TR/TE = 6000/50 ms, slice thickness = 1 mm with no gap, number of slices = 24, number of averages = 2.

Reconstruction: Diffusion weighted (DW) images were first motion and eddy-current corrected using FLIRT part of FSL package (FMRIB Software Library, Oxford, UK). Gaussian smoothing with a FWHM of 0.3mm were then applied to improve the signal-to-noise ratio (SNR). Four DKI reconstruction methods were compared: (1) Conventional NLS method that fits equation [1] first and then solves for the Diffusion tensor D and Kurtosis tensor W through linear equations [2 & 3] (NSL)^{1,4}. (2) Fast DKI reconstruction that explicitly solves $D_{app}(g)$ and $K_{app}(g)$ from equation [1] for exactly 2-bvalues (fDKI)⁵. (3) Tensor-derived method that uses NSL fit for equation [4] directly for tensors D and W (NLS_T). (4) Similar as (3) but solving equation [4] through linear fitting (fDKI_T)⁶. $g = [g_1, g_2, g_3]$ is the unit vector of the applied diffusion direction.

$$\ln(S(g, b)/S_0) = -bD_{app}(g) + \frac{1}{6}b^2D_{app}^2(g)K_{app}(g) \quad [1], \quad D_{app}(g) = \sum_{i=1}^3 \sum_{j=1}^3 g_i g_j D_{ij} \quad [2], \quad K_{app}(g) = \frac{MD^2}{D_{app}(g)} \sum_{i=1}^3 \sum_{j=1}^3 \sum_{k=1}^3 \sum_{l=1}^3 g_i g_j g_k g_l W_{ijkl} \quad [3]$$

$$\ln(S(g, b)/S_0) = -b \sum_{i=1}^3 \sum_{j=1}^3 g_i g_j D_{ij} + \frac{1}{6} b^2 \sum_{i=1}^3 \sum_{j=1}^3 \sum_{k=1}^3 \sum_{l=1}^3 g_i g_j g_k g_l K_{ijkl} \quad [4], \quad \text{Where } K_{ijkl} = MD^2 W_{ijkl} \text{ and } MD = \frac{1}{3} \sum_{i=1}^3 D_{ii}$$

DTI parameters (MD -mean diffusivity, FA -fractional anisotropy) and DKI parameters (MK -mean kurtosis, $K_{//}$ -axial kurtosis, K_{\perp} -radial kurtosis) were calculated^{1,2,7}. As the Kurtosis tensor represent more complex 3D structure, more rigorous formulas were derived to calculate MK and K_{\perp} through surface integration^{5,6} and we refer to those as MK^s and K_{\perp}^s . The complete data set with 5 b-values were fitted voxel-wise using NLS_T and the fitted parametric maps were taken as ground truth. Then a subset of 2 b-values (b = 1000, 2000 s/mm²) were taken out as a short and more clinically practical protocol. All 4 reconstruction methods were tested for the short protocol and resulting parametric maps were compared to the ground truth.

Error analysis: A brain mask was manually drawn to exclude non-brain regions using MIPAV (Medical Image Processing, Analysis, and Visualization) software. The overall percentage error, Err , was calculated as the absolute signal difference with the ground truth map normalized by the sum parameter values:

$$Err = \sum_{i=1}^N |S_i - S_i^{truth}| / \sum_{i=1}^N S_i^{truth} \cdot 100\% \quad [5]$$

N is the total number of voxels within the brain mask. S_i and S_i^{truth} are voxel values within the image for specific method and the ground truth, respectively. Voxels where kurtosis values were negative or too large ($> 3/(b_{max}D)$, where D is diffusivity and b_{max} is the maximum b-value) were excluded (a maximum of 0.7% voxels were observed to have such kurtosis values, e.g. in K_{\perp} map generated from the fDKI method) for fair comparison.

Results: Figure 1 shows generated $K_{//}$, K_{\perp} and K_{\perp}^s maps from all four methods and the ground truth. Both fDKI and NLS produce significantly noisier maps than the tensor derived methods (fDKI_T and NLS_T), especially for the K_{\perp} map (yellow arrows), with NLS performs slightly better than fDKI. Very little differences were observed between the tensor derived methods. The more complex surface integrated version of radial kurtosis, K_{\perp}^s , maps are also less noisy than the K_{\perp} maps. Table 1 shows the calculated overall error, Err , for all four methods and all DTI and DKI related parameters. For DTI related parameters (MD & FA), there is very little difference between the methods. MD is less error prone indicated by a small Err compare to the ground truth. For DKI related parameters ($K_{//}$, K_{\perp} , MK , K_{\perp}^s and MK^s), the tensor derived methods perform significantly better than both fDKI and NLS. NLS produce less error than fDKI as expected by nonlinear fitting, but there is almost no difference between fDKI_T and NLS_T. K_{\perp}^s is less error prone than K_{\perp} as would be expected from the less noisy K_{\perp}^s maps from Figure 1, although MK doesn't show a difference in error compare to MK^s . MK is also a more stable parameter indicated by the lower Err , followed by $K_{//}$ and then K_{\perp} .

Discussion: Tensor derived methods (fDKI_T and NLS) that fit directly for the diffusion and kurtosis tensors (21 parameters) provide better fitting results than the conventional methods (NLS and fDKI) that fit directional diffusivity and kurtosis first (60 parameters for 30 directions) and then reduce to the 21-element tensors. If further constraints for kurtosis value is required, then preference shall be given to tensor derived methods (e.g. as in Tabesh et al.⁶). Among the tensor derived methods, the linear fit (fDKI_T) performs comparable to the more time-consuming nonlinear fit (NLS_T). This may be due to the reduction in fitting parameters in the tensor derived methods compared to conventional methods. For radial kurtosis, one should consider use the more complex surface integrated version for increased accuracy, while for mean kurtosis, an average over K_{app} s from all diffusion directions works as well. Our results suggest that using linear fit for DKI reconstruction with a tensor first approach provides comparable accuracy to nonlinear fit, hence could be the method of choice for faster and more efficient DKI reconstruction.

Reference: [1] Jensen JH, et al. Magn Reson Med. 2005; 53:1432-40. [2] Cheung MM, et al. Neuroimage. 2009. 45:386-92. [3] Falangola MF, et al. J Magn Reson Imaging. 2008. 28:1345-50. [4] Lu H, et al. NMR Biomed. 2006.19:236-247. [5] Jensen JH, et al. NMR Biomed. 2010. 31:741-8. [6] Tabesh A et al. Magn Reson Med. 2010. [7] Wu EX et al. NMR Biomed. 2010. 23:836-48.

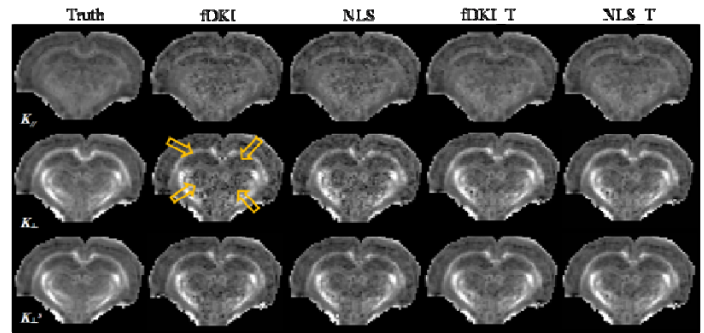


Figure 1. $K_{//}$, K_{\perp} and K_{\perp}^s maps from all four methods (fDKI, NLS, fDKI_T and NLS_T) and the ground truth (Truth).

	fDKI	NLS	fDKI_T	NLS_T
MD	1.99	2.13	1.99	1.99
FA	9.22	9.33	9.22	9.22
$K_{//}$	5.74	4.85	3.38	3.36
K_{\perp}	8.87	8.67	6.13	6.09
MK	70.08	12.48	7.78	7.74
K_{\perp}^s	5.76	4.86	3.38	3.37
MK^s	10.30	8.86	6.05	6.03

Table 1. Calculated overall percentage error, Err , for all four methods and all DTI and DKI related parameters.